Title

K-SHELL IONIZATION IN 7.5- AND 8.6-MeV/a.m.u. U + U COLLISIONS AT VERY SMALL IMPACT PARAMETERS

Author

Molitoris, J.D.

Publication Date

1985-12-01

LBL-21031
Preprint

Lawrence Berkeley Laboratory
UNIVERSITY OF CALIFORNIA

Submitted to Zeitschrift für Physik B

K-SHELL IONIZATION IN 7.5- AND 8.6-MeV/a.m.u. U + U COLLISIONS AT VERY SMALL IMPACT PARAMETERS

J.D. Molitoris, Ch. Stoller, R. Anholt,
W.E. Meyerhof, D.W. Spooner, R.J. McDonald,
L.G. Sobotka, G.J. Wozniak, L.G. Moretto,
M.A. McMahan, E. Morenzoni, M. Nessi,
and W. Wölfli

December 1985

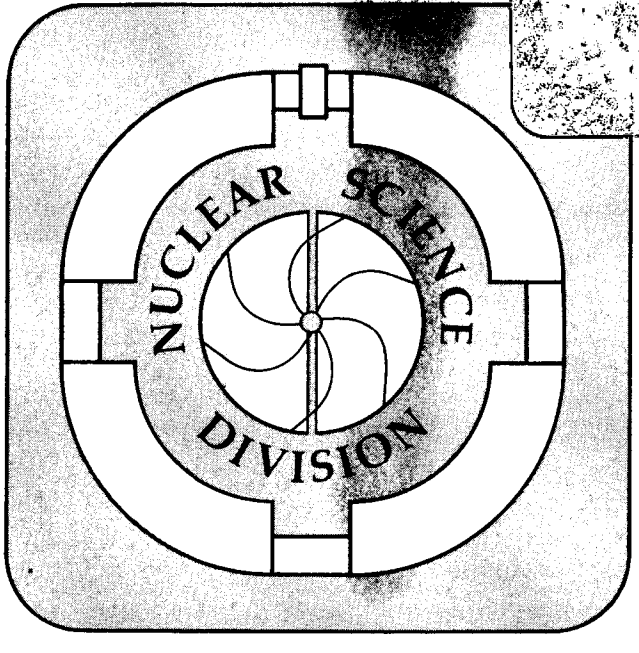

Prepared for the U.S. Department of Energy under Contract DE-AC03-76SF00098

DISCLAIMER

K-SHELL IONIZATION IN 7.5– AND 8.6–MeV/a.m.u. U + U COLLISIONS AT VERY SMALL IMPACT PARAMETERS*

J. D. MOLITORIS, CH. STOLLER,† R. ANHOLT,
W. E. MEYERHOF, D. W. SPOONER

Department of Physics, Stanford University, Stanford CA 94305

R. J. MCDONALD, L. G. SOBOTKA,*
G. J. WOZNIAK, L. G. MORETTO, M. A. MCMAHAN

Nuclear Science Division, Lawrence Berkeley Laboratory, University of California, Berkeley, CA 94720

E. MORENZONI,‡ M. NESSI, W. WÖLFLI

Laboratorium für Kernphysik, Eidg. Technische Hochschule, CH-8093 Zürich, Switzerland

ABSTRACT

K-vacancy production probabilities in elastic 7.5- and 8.6-MeV/a.m.u. U+U collisions are reported for impact parameters less than 15 fm. In 7.5-MeV/a.m.u. U + U collisions the ionization probability rises above the trend indicated by larger impact parameter measurements, increasing to 1.8 vacancies per collision at the smallest impact parameter. The measured probabilities for 8.6-MeV/a.m.u. collisions increase to a maximum value of slightly less than 2 vacancies per collision at the smallest impact parameters. The data is compared to previous results and existing theory.

PACS: 34.50.Fa

---

* Supported in part by the National Science Foundation (Grant PHY-83-13676) and the Department of Energy (Contract No. DE-AC03-76SF00098).

† Presently at the Physics Department, San Jose State University, San Jose, CA 95192.

* Presently at Washington University, St. Louis, MO 63130.

‡ Presently at Swiss Institute for Nuclear Research, CH-5234 Villigen, Switzerland.

I. INTRODUCTION

In previous work [1], we measured K-shell ionization probabilities for U+U collisions at 4.6–, 5.8–, and 7.3–MeV/a.m.u. for impact parameters (b) as large as 85 fm. At the two lower projectile energies the measured ionization probabilities had the same qualitative b dependence (within experimental error) as predicted by coupled-channel calculations [2], but were lower in magnitude. The ionization probability measured at 7.3 MeV/a.m.u. behaved similarly for $b > 20$ fm, but increased above the trend established at large impact parameters for $b < 20$ fm. As this increase in the ionization probability was shown by only two data points, we felt that it deserved further investigation, so we performed measurements for U + U collisions at the slightly higher projectile energy of 7.5–MeV/a.m.u. and at 8.6–MeV/a.m.u. The present measurements at 7.5–MeV/a.m.u. can be considered an extension to smaller impact parameters of the previous measurements at 7.3–MeV/a.m.u., since small differences in the projectile energy have a negligible effect on the K-vacancy production probability.

In the present work, the projectile velocity (v_i) is small compared to the velocity of the K-shell electron (v_e), $v_i/v_e \approx 0.2$, hence the molecular orbital (MO) model should be applicable. In symmetric collisions, both the $1s\sigma$ and $2p\sigma$ MO's correlate to the separated-atom $1s$ level, but K-shell vacancies are produced primarily via the $2p\sigma$ MO since it is less deeply bound than the $1s\sigma$ MO. Studies of K-vacancy production for symmetric collisions at small b, along with related studies in asymmetric collision systems [3], can help to determine the mechanism responsible for K-vacancy production. Some proposed mechanisms for K-vacancy production, such as rotational coupling to higher shells [4,5,6], leave a distinct signature at very small impact parameters. Hence, measurements such as the

present one are important.

A measurement of the K-shell ionization probability at very small impact parameters is also relevant to nuclear time delay studies [7]. In the latter, measurements are made at large scattering angles, but concentrate on x-rays in coincidence with *inelastically* scattered particles. At the same time, one obtains coincidences with *elastically* scattered particles, which allow for a determination of the K-shell ionization probability for zero total kinetic energy loss (TKEL). Such a measurement provides a starting point for a time delay measurement at larger TKEL; in particular, it allows one to estimate the internal conversion contribution to the K x-ray production from nuclear γ-rays [7].

A general difficulty of atomic collisions above the Coulomb barrier is to account adequately for internal conversion due to Coulomb excitation and other nuclear processes. Previously, we used a γ-ray anticoincidence method [8] which worked well in Xe + Pb collisions where the projectile energy exceeded the Coulomb barrier. But, this anticoincidence method does not reject all internal conversion events due to Coulomb excitation. In our previous U + U collision studies [1], with the γ-ray anticoincidence condition in effect, the unrejected x-ray yield from nuclear Coulomb excitation never amounted to more than 17% of the atomic K x-ray yield. In the present work, which did not use the anticoincidence method, the x-ray yield due to internal conversion from Coulomb excitation was as large as 33% of the atomic K x-ray yield at the largest scattering angles. This increase in the internal conversion contribution to the K x-ray yield is probably due to the absence of the anticoincidence condition. Although the anticoincidence technique helped to eliminate some γ-ray internal conversion effects in our U + U collision studies [1], we determined that a measurement of the K-vacancy

production probability in U + U collisions could be made without it.

Another difficulty in the present measurements is due to the fact that they are made at projectile energies above the Coulomb barrier and at rather large scattering angles where nuclear reaction effects can increase the internal conversion contribution to the K-vacancy production in addition to that of nuclear Coulomb excitation. We discuss these and other difficulties below in Sect. III. Section II describes our experiment and details of the method used. In Sect. IV we present and discuss our results.

II. EXPERIMENT

A. Apparatus

Beams of ^{238}U ions with energies of 7.5– and 8.6–MeV/a.m.u. from the Lawrence Berkeley Laboratory SuperHILAC bombarded 683- and 750-μg/cm^2 ^{238}U targets which were placed perpendicular to the beam. Figure 1 is a schematic diagram of our experimental set–up. We detected scattered particles in a large-solid-angle radial ionization chamber [9] which was centered at $\theta_{LAB} = 40°$ and subtended an angular range of $\pm$ 14.5°. The ionization chamber is position sensitive for both in-plane (θ) and out-of-plane (ϕ) angles and has three energy loss sections (ΔE_1, ΔE_2, and E_{REST}). The pressure of an argon – 10% methane gas mixture in the ionization chamber was adjusted to stop the highest energy scattered particle in the E_{REST} section of the detector. The collision partners of the particles detected in the ionization chamber were detected in a parallel plate avalanche counter (PPAC) which was positioned at 45° on the other side of the beam and which subtended an angular range of $\pm$ 20° in θ_{LAB}. X-rays

were detected at 135° to the beam direction (opposite the PPAC, in the particle detector plane) by an 800-mm^2 by 8-mm thick intrinsic Ge detector with a pulsed-optical feedback preamplifier. A coaxial Ge(Li) detector at 130° to the beam (opposite to the ionization chamber) measured the higher energy γ-rays from Coulomb excitation and nuclear processes.

Absorbers were placed in front of the intrinsic Ge detector (0.254 mm Ni, 0.508 mm Cd) and Ge(Li) detector (1.600 mm Cd, 0.889 mm Cu) to reduce the count rate from low energy photons. The efficiency and solid angle of these detectors were determined by placing calibrated radioactive sources at the target position. The dead-time correction for the preamplifier, amplifier, and pile-up rejector was determined by sending electronic pulses into the detector preamplifier. Counting rates were corrected by the ratio of the number of pulses sent into the preamplifier to the number of pulses found in the pulser peak of the calibration spectra.

Data was recorded in event mode on the LBL Modcomp Classic computer. A valid event consisted of a triple coincidence between the PPAC, ion chamber, and at least one of the photon detectors. For each event, we recorded: x-ray energy (intrinsic Ge detector), γ-ray energy (Ge(Li) detector), particle energies in the ionization chamber (ΔE_1, ΔE_2, and E_{REST}), and position in the ionization chamber (θ_{IC}, ϕ_{IC}). As the PPAC generated a master start signal for each event, the following time spectra were also recorded: PPAC-IC (ionization chamber), PPAC-X (intrinsic Ge), and PPAC-γ (Ge(Li)). A scaled down number of particle single events which did not require a particle – x-ray coincidence were simultaneously recorded.

B. Method

We used the x-ray – particle coincidence method to determine vacancy production probabilities [10], but instead of varying the angle of a particle detector we used a large-solid-angle position sensitive ionization chamber. For our evaluation, we divided the θ acceptance of the ionization chamber into eight θ-bins. The three ΔE sections of the ionization chamber were then calibrated by varying the beam energy below the Coulomb barrier and observing elastically scattered U particles from U and lower-Z targets. This calibration allowed us to calculate the total energy of the detected particle. The particle energy spectrum exhibited the usual "quasi-elastic" peak, which is composed of true elastically scattered particles and slightly inelastic events which extend into the elastic region [11,12]. For each angle we then subdivided the highest energy, mostly elastic part of the particle energy spectra into energy bins and compared the number of particle - x-ray coincidences corresponding to each bin. When we had determined a bin size such that the ratios of the x-rays to particles was constant over at least the three highest energy bins, we summed over these bins to determine the K-vacancy production probability due to atomic excitation. This technique is described in greater detail in [1] and [8].

The ionization chamber was designed so that, provided the beam spot was sufficiently small, incident particles in the central plane of the detector traversed the active region of the detector radially with path lengths in the ΔE sections independent of θ_{LAB}. Collimation in θ_{LAB} and proper gating during the analysis eliminated edge effects. The detector was collimated in the azimuthal angle, so that incident particles originating from the target center traversed and stopped in the active region of the detector. In the analysis, we required that particles

detected in the ionization chamber register signals in the three energy loss sections in addition to having the correct ΔE_1 and ΔE_2 for a scattered U particle. In this way we could discriminate against fission fragments and other lower-Z particles formed by quasi-elastic nuclear reactions. By simultaneously gating on the time difference between the PPAC and ionization chamber *and* on the time difference between the PPAC and x-ray detector we established the particle – x-ray coincidence. We also counted the random coincident x-rays and subtracted their number from the coincident x-ray yield (this correction was less than 5% for all angles).

III. DATA REDUCTION

A major problem in measuring the ionization probability for symmetric collisions is that in general one can determine only a dominant center-of-mass scattering angle and impact parameter [1]. Each collision involves x-rays emitted from the primary scattered particle (detected in the ion chamber) and x-rays emitted from the collision partner (detected in the PPAC). At some angles, due to our geometry, we can separate these x-rays by their different Doppler shifts (see Figure 2a), but it is still impossible to determine a unique center-of-mass angle and impact parameter for the collision. For laboratory angles smaller than 45°, most of the particles detected in the ionization chamber are, in fact, scattered projectiles and most of the collision partners are target recoil atoms (from $\Theta_{CM} = 2\theta_{LAB}$). However, a fraction of the particles detected in the ion chamber are recoil target ions coming from the other center-of-mass angle, $\Theta_{CM} = \pi - 2\theta_{LAB}$. As θ_{LAB} increases beyond 45° this situation reverses and we detect mainly target recoils. The only angle where the impact parameter for the collision is unique is

$\theta_{LAB} = 45°$, because here both center-of-mass angles are the same. Furthermore, in symmetric Coulomb scattering collisions the dominant center-of-mass angle is always the smaller one, so particles detected at laboratory angles greater than 45° come predominantly from $\Theta_{CM} = \pi - 2\theta_{LAB}$ and hence the smallest impact parameter which can be determined is from $\theta_{LAB} = 45°$. Our measured ionization probabilities are always plotted vs. the impact parameter of the dominant center-of-mass angle.

All our measurements were made at projectile energies above the Coulomb barrier ($\sim$ 5.17 MeV/a.m.u. for U + U). In addition, some measurements were made beyond the grazing angle for nuclear reactions (also called the quarter-point angle as it is the angle where the cross section for elastic scattering has decreased to one quarter of its Rutherford value due to the onset of nuclear reactions: $\theta_{LAB}^{1/4} \approx 44.5°$ for 7.5 MeV/a.m.u. and $\theta_{LAB}^{1/4} \approx 34.7°$ for 8.6 MeV/a.m.u.). Nuclear reactions tend to make the contribution from the larger center-of-mass angles virtually extinct, so elastic scattering from the smaller center-of-mass angles is more dominant. As the laboratory scattering angle goes beyond its $\theta_{LAB}^{1/4}$ value, we observed significant reductions in the cross section for elastic scattering. Hence, one must make a careful calibration of the total particle energy spectra, so that the gated particles are indeed in the energy region where elastically scattered particles are expected.

Figure 2 shows x-ray spectra coincident with elastically scattered particles at two different angles. In the spectrum coincident with particles in the ionization chamber at $\theta_{LAB} = 27°$, the Doppler effect does not shift the observed x-rays of the primary scattered particle and those of its collision partner apart enough to resolve separate K x-ray lines. However, for the x-rays coincident with particles

at $\theta_{LAB} = 53°$, the Doppler shift is enough to separate the $K\alpha$ x-rays of the primary scattered particle (unprimed in the figure) from those of its collision partner (primed). The latter spectrum also shows that the intensity of both these x-ray lines are equal, as it should be for symmetric collisions (the $K\alpha$ peak appears slightly wider than $K\alpha'$ as some $K\beta'$ x-rays are mixed in). In addition to the $K\alpha$ and $K\beta$ x-ray lines of U, these spectra show Coulomb excited γ-lines which we use to estimate internal conversion and a γ-ray continuum caused by nuclear reactions and Compton scattering in the detector. The two lowest energy γ-rays are not seen in Fig. 2. The γ_1 line is highly converted in the L-shell and cannot be seen above the background. The γ_2 line is slightly visible as a spur on the high energy side of the $K\alpha$ line and as it is usually inseparable from the K x-rays we must estimate its yield and subtract it [1]. The small peak on the low-energy side of the U $K\alpha$ x-rays in both spectra is an un-Doppler shifted Pb x-ray line due to fluorescence in the shielding around the x-ray detector.

Problems associated with the analysis of these particle-coincident U x-ray spectra and the determination of the internal conversion due to Coulomb excitation are thoroughly discussed in our previous paper [1]. However, here we must also consider additional sources of internal conversion since any photon with an energy greater than the K-shell binding energy (115.59 keV for U) can convert in the K-shell.

Normally, when measuring K-vacancy production probabilities one has to account only for the internal conversion from discrete Coulomb excited γ-lines. However, for large scattering angles and projectile energies above the Coulomb barrier, nuclear reactions also cause a γ-ray continuum to be present in the x-ray energy spectra (with their Compton background). Unfortunately, the internal

conversion from this background can be significant for measurements of the ionization probability at the smallest impact parameters.

In order to account for the internal conversion of γ-rays from quasi-elastic reaction products that are mixed in with the elastically scattered particles, we use a technique from our time delay studies [7]. First, the K-vacancy yield due to internal conversion is determined for events in which Coulomb excitation dominates (x-rays coincident with scattered particles at $\theta_{LAB} = 27°$ and 30°). We note that at larger scattering angles the general shape of the x-ray spectra above the K-absorption edge is the same as at smaller scattering angles, except that the Coulomb excitation lines are not as pronounced (due to the increased continuum and the Doppler splitting discussed above). We now make the assumption that the amount of internal conversion (P_{IC}) is proportional to the total number of γ-rays (N_γ) measured with energies above the K absorption edge: $P_{IC} = cN_\gamma$, where c is determined from those scattering angles where Coulomb excitation in elastic collisions dominate. This method assumes that the mean conversion coefficient of the γ-rays is independent of any TKEL in the collision, an assumption which should be reasonable as the multipolarity of the dominant γ-rays is E2 [13]. This method accounts for an increased number of quasi-elastic events which mix in with the elastic events at small b.

IV. RESULTS AND DISCUSSION

In Figs. 3 and 4 we plot the measured K-vacancy production probabilities as a function of the impact parameter (in fm). We assume Rutherford scattering to convert scattering angles to impact parameters, always plotting the impact parameter associated with the dominant center-of-mass scattering angle. The probabilities are determined from the total atomic U K x-ray yield and represent the sum of $2p\sigma$ and $1s\sigma$ MO ionization.

Errors in the measured probabilities are limited to statistics and uncertainties from the internal conversion estimate. There is also some uncertainty in the assigned impact parameters (not shown), which is due to the finite width of each θ-bin in the ionization chamber. The probabilities are plotted vs. b corresponding to the central angle of each bin.

A. U + U Collisions at 7.5 MeV/a.m.u.

In Fig. 3, we compare present results for 7.5 MeV/a.m.u. with those of our previous experiment at 7.3-MeV/a.m.u. [1]. The agreement between both experiments is quite good in the region of overlap. Differences in the two data sets are probably due to differences in the x-ray detector efficiency calibration (which can vary as much as $\pm$ 15%). The three lowest impact parameter points of the 7.3 MeV/a.m.u. data have been corrected here as the background and internal conversion contribution for them was underestimated in the previous paper [1].

The present data confirms that there is a marked increase in the ionization probability for very small b. In fact, the measured probability increases to 1.8 vacancies per collision at the smallest impact parameter. As there are two uranium

atoms in the collision, up to four K-vacancies can be created and the maximum value the K-shell ionization probability can have is four.

Figure 3 also compares available theoretical calculations of the K-vacancy production probability for U + U collisions at 7.5 MeV/a.m.u. with the data The solid line is a coupled-channel calculation by Reinhardt [14], which includes only $1s\sigma$ and $2p_{1/2}\sigma$ states (bound and continuum) interacting via radial coupling. This calculation is in qualitative agreement with the data for $b \leq 8$ fm, however, it does not reflect the increase at small b. The theoretical probabilities have the same qualitative impact parameter dependence for $b > 20$ fm as our previous data [1], but exceed them by a factor of about 1.6. It has been suggested [14] that the disagreement between the coupled channel calculations and experiment is due to the neglect of other channels. The small b behavior then could be due to rotational coupling via $2p_{3/2}\pi$, $2p_{3/2}\sigma \rightarrow 2p_{1/2}\sigma$ MO's.

The dashed-dotted line in Fig. 3 is an extrapolation of a theoretical calculation by Heiligenthal *et al.* [4], which does attempt to account for the influence of rotational coupling. This is a calculation of $2p\sigma$ vacancy production including direct ionization and the coupling of a $2p_{3/2}$ vacancy into the $2p_{1/2}$ (σ) MO. The original calculation was done for $2p_{1/2}\sigma$ vacancy production in 4.7-MeV/a.m.u. U + U collisions. We have adjusted the impact parameter dependence of this theory to the larger bombarding energy of 7.5-MeV/a.m.u. and arbitrarily scaled it up by a factor of 4 to compare with our data. Strictly speaking, the $1s\sigma$ ionization probability should be subtracted from the data (one can estimate this from the scaling law) to compare with this theory, but subtracting the $1s\sigma$ contribution here does not change the character of the data. This calculation does predict an increase in the ionization probability at small b, but not as steep as

the measurements indicate. Also it does not predict the b dependence well for $b > 25$ fm.

The dashed line in Figure 3 is the result of a scaling law calculation which we have found to be reasonably accurate at larger impact parameters and also in lower energy U + U collisions [1]. The scaling law [15,16] gives the K-vacancy production probability, P_{KV}, as a function of $R_0(b)q_0$, where R_0 is the distance of closest approach in the collision and

$$q_0 = E_K(R_0)/\hbar v_i \ . \tag{1}$$

Here E_K is the binding energy of the $2p\sigma$ or $1s\sigma$ MO and v_i is the ion velocity. The scaling law takes the form:

$$P_{KV} = F(Z_U)\ \exp\ (-m\ R_0 q_0)\ . \tag{2}$$

Armbruster *et al.*[17] have shown that $m = 2$ for $1s\sigma$ ionization in asymmetric collisions; for $2p\sigma$ ionization in Pb + Cm collisions $m = 2.5$ gives good agreement with their data over a range of energies from 3.6- to 5.9-MeV/a.m.u.

We use the scaling law to calculate $P_{1s\sigma}$ and $P_{2p\sigma}$ for U + U collisions and then sum these two probabilities to compare with our results. For $1s\sigma$ excitation we take $m = 2$ and $F(Z_U = 184) = 2$ [16]. We also chose $m = 2$ for $2p\sigma$ excitation here as it seems to fit these and other results [1,3] better than $m = 2.5$. For $2p\sigma$ ionization, we take $F(Z_U) = 2.39(\pm 0.40)$, a value we determined to be constant over projectile energies from 4.6- to 7.3-MeV/a.m.u. in U + U collisions [1]. The method of Soff *et al.*[18] is used to obtain the MO binding energy E_K in Eq. (1). The resultant scaling law calculation is in agreement with the larger b data, but does not reflect the small b behavior of the present data.

B. U + U Collisions at 8.6 MeV/a.m.u.

In Fig. 4, we plot the measured K-vacancy production probabilities for 8.6 MeV/a.m.u. U + U collisions. The increased uncertainty in some of the probabilities is due to the onset of nuclear reactions which reduces the elastic scattering cross section. The data reaches a maximum probability of a slightly less than 2 vacancies per collision for $b < 8$ fm. The decrease in P_{KV} at $b = 6.6$ fm. is not statistically significant. As b increases, the probability falls off less rapidly than it does for 7.5-MeV/a.m.u. collisions.

The dashed line is from a scaling law calculation, where again we calculate the probability for $2p\sigma$ and $1s\sigma$ ionization and sum to compare with our data. The same values for m and F are used here as above. At this projectile energy, the scaling law falls below the data, but seems to converge with the data as b increases. The solid line is a coupled-channel calculation [14] which agrees with the data at the smaller impact parameters, but does not reflect the general trend.

The dashed-dotted line in Fig. 4 is an extrapolation of the calculation by Heiligenthal *et al.*[4] to 8.6 MeV/a.m.u., scaled up by a factor of 5. From $b = 6$ to about 9 fm, this calculation fits the trend of the data well, but as b increases the measured ionization probabilities fall off faster than the theory.

The real significance of Heiligenthal's calculation is its behavior for $b < 6$ fm (not shown in Fig. 4), where it predicts a drop in the ionization probability of about 63% from $b = 5.5$ to 0 fm. This behavior is caused by the inclusion of strong rotational and radial couplings between substates of the quasimolecular L-shell. Unfortunately, it is not possible for us to measure the ionization probability for $b < 6$ fm in these symmetric collisions. This is due to the difficulties outlined above in the scattering of identical particles, but the onset of nuclear

reactions also precludes such a measurement. However, in U + Pb collisions at 4.7-MeV/a.m.u. Greenberg *et al.*[19] observed a drop in the $2p\sigma$ ionization probability of about 26% for laboratory angles from 29° to 47°. This is within the angular range of the present measurements, but for U + U we observe no decrease in the ionization probability. Furthermore, in a previous measurement for U + Pb collisions at 4.6-MeV/a.m.u. [1], the $2p\sigma$ ionization probability was observed to increase from $\theta_{LAB} = 25°$ to 35°. The experimental technique used by Greenberg *et al.* was based on K x-ray line shape measurements which takes advantage of the Doppler shift of the emitted target K x-rays when K vacancies are produced in small impact parameter collisions. They observed a similar decrease for $1s\sigma$ vacancy production in Xe + Pb collisions [19] which was also not observed by particle-x-ray coincidence techniques [20].

Figure 5 is a summary of all the $2p\sigma$-ionization probability data for elastic U + U collisions from present work and [1]. Here we used the scaling law to calculate the $1s\sigma$ ionization probability for these collisions and then subtracted $P_{1s\sigma}$ from the measured total K-shell ionization probability. As most of the measured probability is due to $2p\sigma$ ionization, this allows us a good estimate of the $2p\sigma$ ionization probability ($P_{2p\sigma}$). In Fig. 5, $P_{2p\sigma}$ is plotted against R_0q_0, where q_0 is determined from Eq. (1) with $E_K = E_{2p\sigma}$. Although the agreement is not excellent, the data appears to follow a common trend for $R_0q_0 > 0.6$. The solid line is Eq. (2) with $F = 2.39$ and $m = 2$. The dashed line is also Eq. (2), but with $F = 3.32$ and $m = 2.5$. Although the $m = 2.5$ line fits the central body of the data well, it disagrees with the data at both extremes. The $m = 2$ line fails only for $R_0q_0 < 0.6$, where $P_{2p\sigma}$ appears to be enhanced.

V. CONCLUSIONS

The present data for 7.5- and 8.6-MeV/a.m.u. U+U collisions indicates an enhancement of the K-vacancy production probability for very small b (< 10 fm). The measured ionization probabilities increase to 1.8 vacancies per collision for 7.5-MeV/a.m.u. U + U collisions and to just below 2 vacancies per collision for projectile energies of 8.6 MeV/a.m.u.

Although scaling law calculations under-estimate the present very small impact parameter data, there is overall agreement with the scaling law for all available high-energy U+U ionization probability measurements. Coupled channel calculations [2,14] do not predict the b dependence of the ionization probability well for very small b, although there is some qualitative agreement here and for larger b [1].

One possible mechanism explaining the small b behavior of these ionization probabilities could be the influence of rotational coupling of vacancies created in higher MO's to the $2p\sigma$ MO [14], but the coupled-channeled calculation of Heiligenthal *et al.* [4], which assumes the presence of the $2p_{3/2}$ vacancy, is about a factor of 4 below experiment. Since probably much fewer than one $2p_{3/2}$ vacancy is available during the collision, this is an upper limit. In addition, when normalized to the data this calculation exceeds the experimental results at large b.

ACKNOWLEDGEMENTS

The authors would like to thank Dan Semides (Stanford) for his skillful machining of various pieces of the apparatus and Wolfgang Jung and Ed Dillard of Stanford for their technical assistance. The mechanical and technical assistance of Bill Elwood and the SuperHILAC support staff was most appreciated during the upgrading of the "M" cave to a photon-particle coincidence facility. This work was supported in part by the National Science Foundation, Grant PHY 83-13676 and by the Director, Office of Energy Research, Division of Nuclear Physics of the Office of High Energy and Nuclear Physics of the U.S. Department of Energy under Contract No. DE-AC03-76SF00098.

REFERENCES

1. Molitoris, J. D., Anholt, R., Meyerhof, W. E., Baker, O. K., Andriamonje, S., Morenzoni, E.: Z. Phys. A – Atoms and Nuclei (to be published).
2. deReus, T. H. J., Müller, U.: (private communication, 1984).
3. Anholt, R., Spooner, D., Molitoris, J. D., Stoller, Ch.: Submitted to J. Phys. B. Letters (1985).
4. Heiligenthal, G., Betz, W., Soff, G., Müller, B., Greiner, W.: Z. Phys. A – Atoms and Nuclei 285, 105 (1978).
5. Briggs, J. S., Macek, H. H.: J. Phys. B5, 579 (1972).
6. Mann, M., Mokler, P. H., Fricke, B., Sepp, W-D., Shoenfeldt, W. A., Hartung, H.: J. Phys. B15, 4199 (1982).
7. Stoller, Ch., Nessi, M., Morenzoni, E., Wölfli, W., Meyerhof, W. E., Molitoris, J. D., Grosse, E., Michel, Ch.: Phys. Rev. Lett. 53, 14, 1329 (1984).
8. Anholt, R., Meyerhof, W. E., Molitoris, J. D., Xu, J-S.: Z. Phys. A – Atoms and Nuclei 308, 189 (1982).
9. Sobotka, L. G., Hunter, J. B., Wozniak, G. J.: Lawrence Berkeley Laboratory Report No. LBL-16870, 267 (1984).
10. Liesen, D., Armbruster, P., Behncke, H. -H., Hagmann, S.: Z. Phys. A – Atoms and Nuclei 288, 417 (1978).
11. Schroeder, W. U., Huizenga, J. R.: Ann. Rev. of Nucl. Sci. 27, 465 (1977).
12. Birkelund, J. R., Huizenga, J. R., Freiseleben, H., Wolf, K. L., Unik, J. P., Viola, V. E., Jr.: Phys. Rev. C 13, 133 (1976).
13. Aguer, P., Schmitt, R. P., Wozniak, G. J., Habs, D., Diamond, R. M., Ellegaard, C., Hillis, D. L., Hsu, C. C., Mathews, G. J., Moretto, L. G.,

Rattazzi, G. U., Roulet, C. P., Stephens, F. S.: Phys. Rev. Lett. 43, 1778 (1979).

14. Reinhardt, J.: (private communication, 1985).

15. Müller, B., Soff, G., Greiner, W., Ceausescu, V.: Z. Phys. A – Atoms and Nuclei 285, 7 (1978).

16. Bosch, F., Liesen, D., Armbruster, P., Maor, D., Mokler, P. H., Schmidt-Böcking, H., Schuch, R.: Z. Phys. A – Atoms and Nuclei 296, 11 (1980).

17. Armbruster, P.: in Quantum Electrodynamics of Strong Fields, (Greiner, W. ed., Plenum, New York), p. 189 (1983).

18. Soff, G., Reinhardt, J., Betz, W., Rafelski, J.: Physica Scripta, Vol. 17, 417 (1978).

19. Greenberg, J., Bokemeyer, H., Emling, H., Grosse, E., Schwalm, D., Wollersheim, H. J., Bosch F.: X ICPEAC, Abstracts of Papers (Paris, 1977), p. 160 and Phys. Rev. Lett. 39, 1404 (1977).

20. Anholt, R., Meyerhof, W. E., Stoller, Ch.: Z. Phys. A–Atoms and Nuclei 291, 287 (1979).

Figure Captions

1. Schematic of experimental set-up. The PPAC is a parallel plate avalanche counter. ΔE_1, ΔE_2, and E_{REST} refer to the three energy sections of the ionization chamber.

2. X-rays in coincidence with elastically scattered particles from 7.5-MeV/a.m.u. U + U collisions. The inset diagrams illustrate the different scattering situations. **a.** At $\theta_{LAB} = 53°$ the Doppler shift splits the x- and γ-rays emitted from each partner in the collision. Unprimed quantities are emitted from particles detected in the ionization chamber. **b.** At $\theta_{LAB} = 27°$ the Doppler shift is not large enough to split the x- and γ-ray lines from the collision partners.

3. K-vacancy production probabilities for elastic U + U collisions at 7.5-MeV/a.m.u. as a function of the impact parameter (• present work, ○ data of [1] for 7.3-MeV/a.m.u. U+U collisions). The solid line is a coupled channel calculation [2] and the dashed line is a fit using a scaling law [13,14]. The dashed-dotted line is a scaled up (×4) extrapolation of a calculation [4] which attempts to account for the influence of rotational coupling.

4. K-vacancy production probabilities in 8.6-MeV/a.m.u. elastic U + U collisions as a function of the impact parameter. The solid line is a coupled channel calculation [14] and the dashed-dotted line is an extrapolation of a calculation for lower energy U + U collisions [4] to this energy, which is scaled up (×5). The dashed line is the result of a fit to the data using a scaling law [13,14].

5. Summary of the measured $2p\sigma$-ionization probabilities for elastic U+U collisions from [1] and present work. The scaling law, Eq. (2), is used to subtract the $1s\sigma$ contribution. The solid line is Eq. (2) for $2p\sigma$ ionization with $F = 2.39$ and $m = 2.0$ while the dashed line has $F = 3.32$ and $m = 2.5$. The extended (dashed) error bars on some data points are explained in [1].

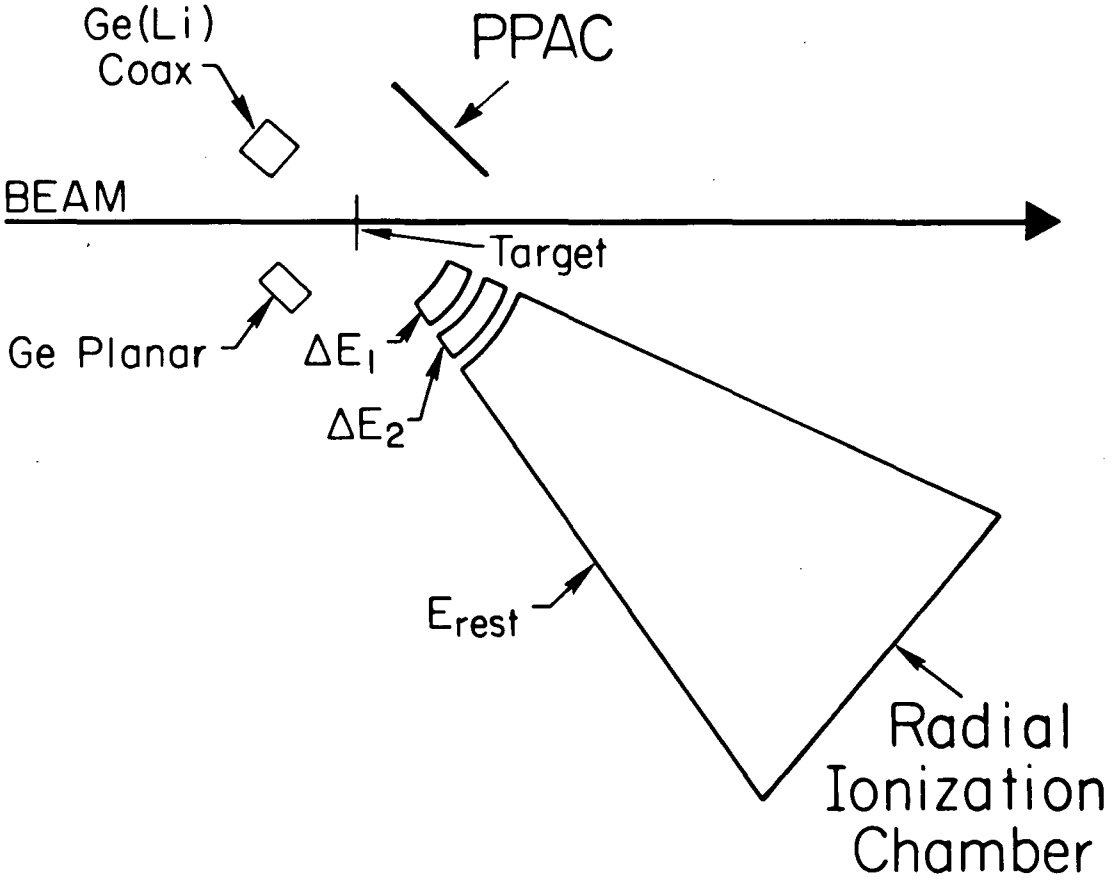

XBL 862-379

FIG. 1

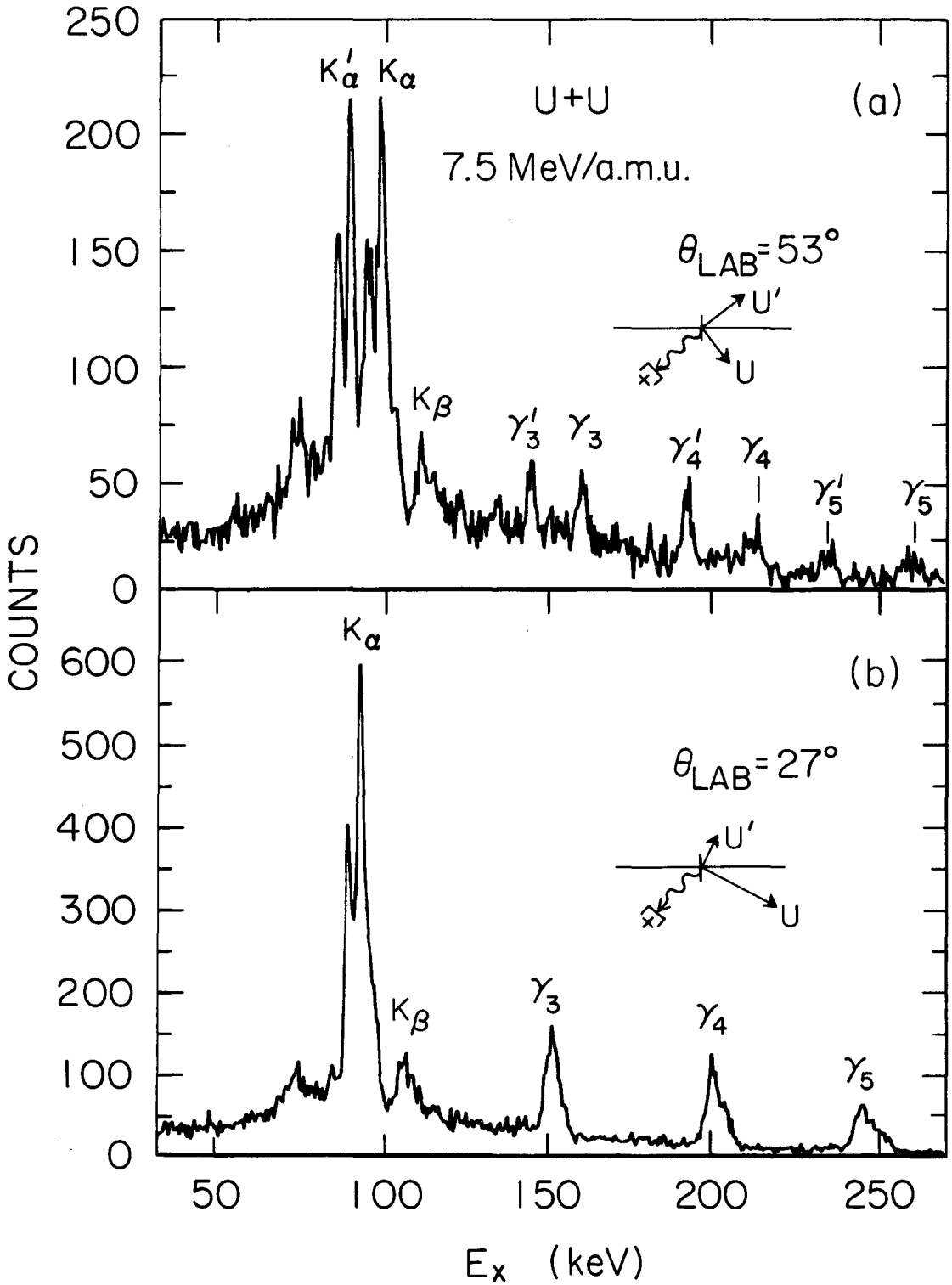

XBL 862-375

FIG. 2

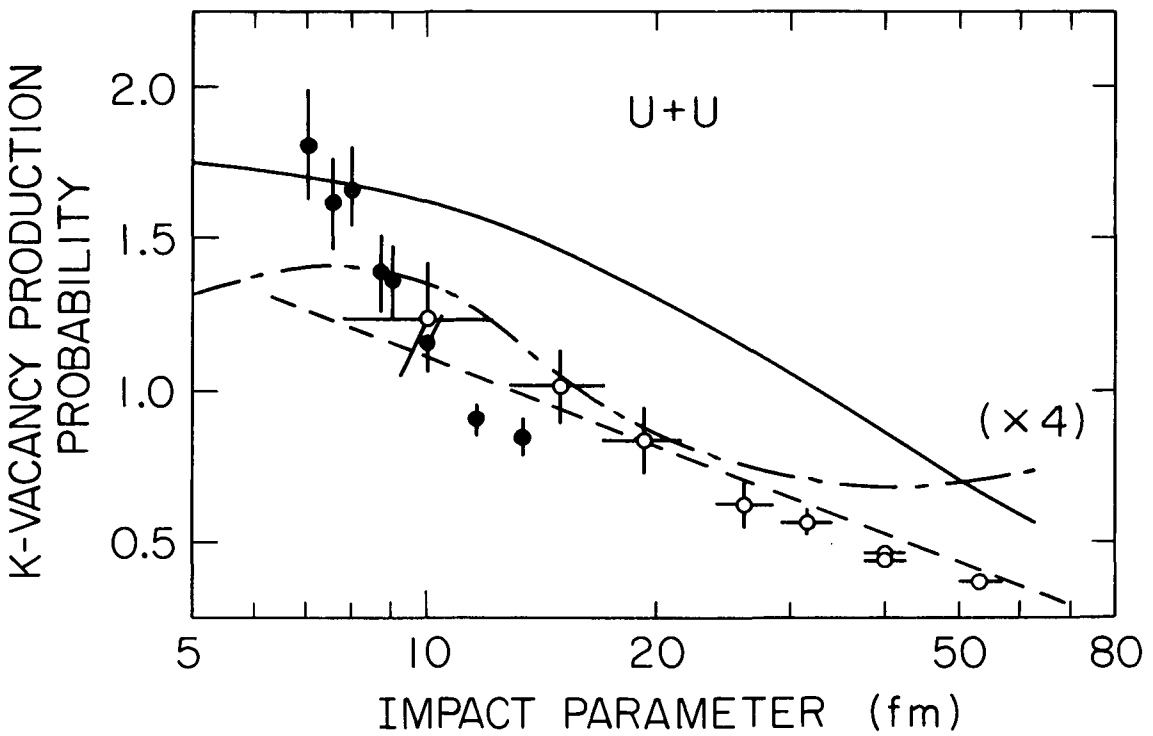

XBL 862-378

FIG. 3

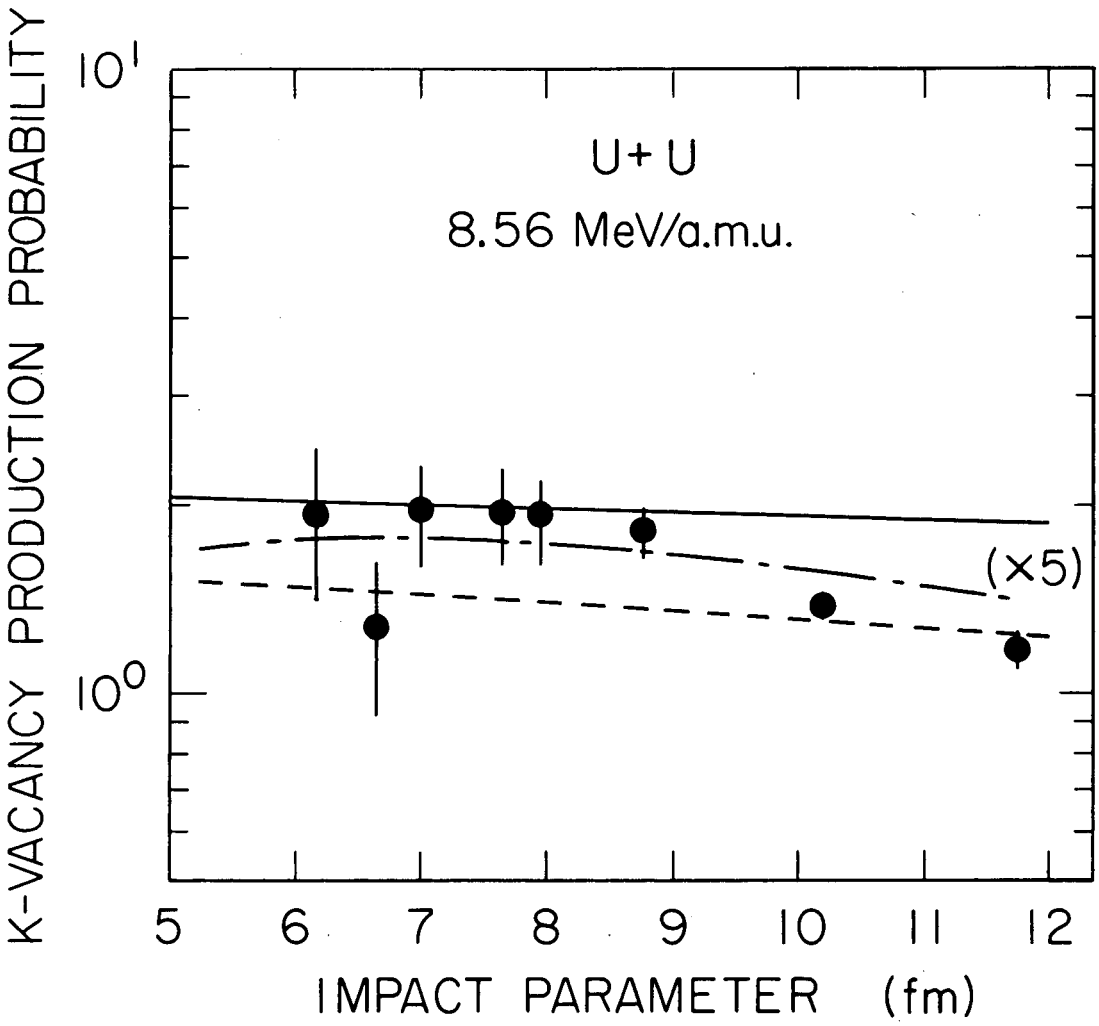

XBL 862-376

FIG. 4

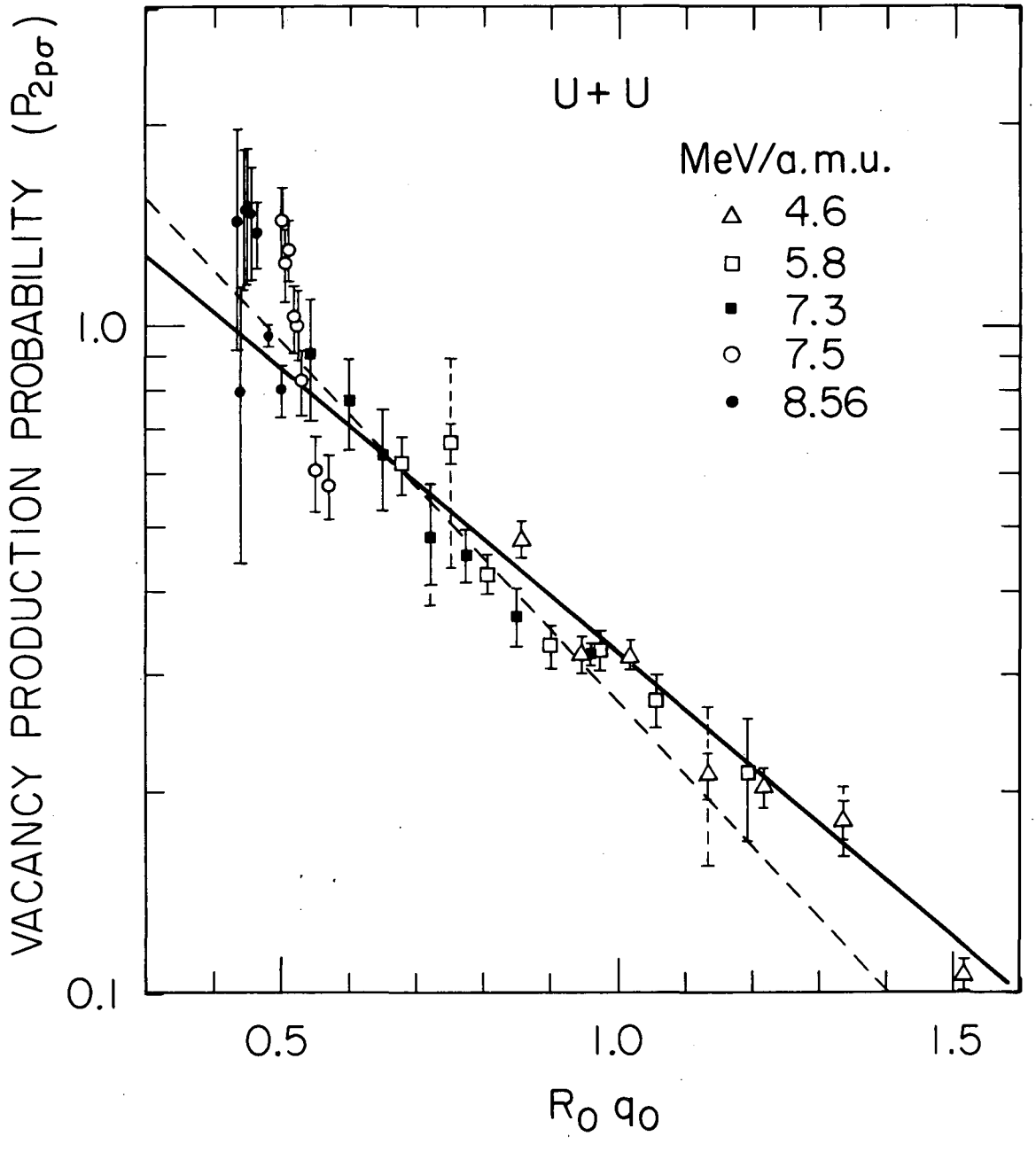

XBL 862-377

FIG. 5

This report was done with support from the Department of Energy. Any conclusions or opinions expressed in this report represent solely those of the author(s) and not necessarily those of The Regents of the University of California, the Lawrence Berkeley Laboratory or the Department of Energy.

Reference to a company or product name does not imply approval or recommendation of the product by the University of California or the U.S. Department of Energy to the exclusion of others that may be suitable.

LAWRENCE BERKELEY LABORATORY
TECHNICAL INFORMATION DEPARTMENT
UNIVERSITY OF CALIFORNIA
BERKELEY, CALIFORNIA 94720